Continental J. Applied Sciences 8 (2): 7 - 25, 2013 ISSN: 1597 – 9928
© Wilolud Journals, 2013 http://www.wiloludjournal.com
Printed in Nigeria doi:10.5707/cjapplsci.2013.8.2.7.25

FRACTAL CHARACTERIZATION OF BASEMENT TOPOGRAPHY: APPLICATION TO PARTS OF SOUTHERN BIDA BASIN, NIGERIA AND THE SURROUNDING BASEMENT ROCKS

John U. Megwara[1] and Emmanuel E. Udensi[2]
[1]Nigerian Geological Survey Agency, P.M.B. 2007, Kaduna, Nigeria
[2]Federal University of Technology, P.M.B.65, Minna, Nigeria

ABSTRACT
Determination of basement relief using fractal method was carried out over parts of southern Bida basin, Nigeria and the surrounding basement rocks. The research covered both basin and basement rock sections. The number of data points used for analysis were 2,937, obtained from the digitization of eleven ½ degrees by ½ degrees aeromagnetic contour maps. Data processing methods used in the study include regional–residual separation of the total magnetic intensity data, determination of depth–to–top and depth–to–bottom of magnetic sources and estimation of source scaling exponent using the Fractal technique. The research gave the thickness of sediments ranging from 0.022 km at Katakwa in the south–eastern part; to 3.88 km at Lafiagi in the north–western section of the survey area, thus depicting the topography of the basement rock.

KEYWORDS: Basement, basin, fractal, magnetics, topography

Received for Publication: 13/11/12 Accepted for Publication: 21/01/13
Corresponding Author: megwarauj@yahoo.com

INTRODUCTION

Quantitative interpretation of magnetic data includes estimating dip, susceptibility, and depth associated with the sources of an anomalous magnetic response. Methods exist for estimating depth using either data recorded along a profile or data interpolated onto a regular grid. The advantage of the latter approach is that the resulting images are relatively simple and quick to produce regional structural patterns, and are easily overlain on other geophysical and geological maps (Thurston *et al*., 2002). Thurston and Smith (1997) used the local wavenumber to estimate the depth of 2-dimensional thin sheets and contacts; using a priori information to determine which model is more appropriate. This method was subsequently generalized by introducing the concept of a multimodel wavenumber (Smith *et al*., 1998).The term multimodel applies because this quantity gives the same result regardless of whether the source is a horizontal cylinder, a thin sheet, or a contact. In this study, estimation of the depth-to-top of magnetic sources is achieved by employing a fractal characterization technique.

Geology of the study area

The study area shown in Figure 1, is bounded by longitudes 4.5° E to 8.0° E and latitudes 8.0° N to 9.0° N. The geology of the study area is shown in Figure 2; marked out in black outline. The southern Bida basin section of the study area forms a part of the larger Bida basin. The successions in the southern Bida basin consist of the basal Lokoja Formation, overlain by the Patti Formation and capped by the Agbaja Formation. The basal Lokoja Formation is a sequence of matrix supported conglomerates and sandstones overlying the Pre–Cambrian to lower Paleozoic basement. Depositional environments are predominantly within fluvial systems of a continental setting. The Patti Formation consists of dark grey carbonaceous shales; mudstones and siltstones representing flood plains to shallow marine deposits with likely organic rich intervals. The overlying Agbaja Formation is made up of ferruginised oolitic and kaolinitic mudstone of a marginal environment (Akande *et al*., 2005). The surrounding Pre–Cambrian basement rocks consist of a suit of Pre–Cambrian gneisses, migmatites and metasedimentary schist crosscut by intrusive granitoids (Shekwolo, 1992).The Pre–Cambrian basement rocks experienced severe deformation during the late Pan–African phase (600 m.y.), and developed megashears that were reactivated during the late Campanian–Maastrichtian (Braide,1990). The gneisses and metasedimentary schist are found mostly as flat lying outcrops (Shekwolo, 1992).

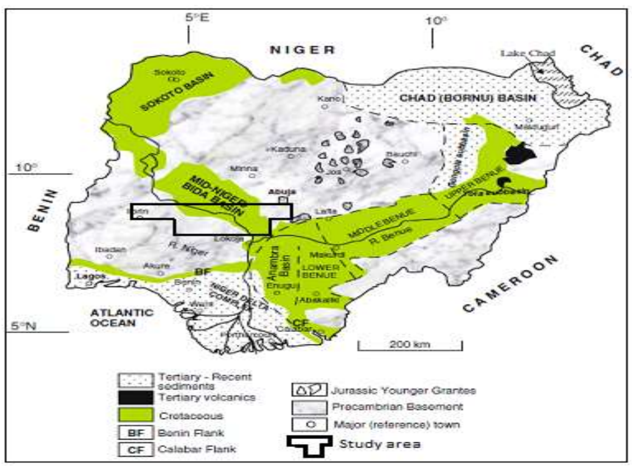

Fig. 1 Geological map of Nigeria showing the study area (Source: Obaje, 2009)

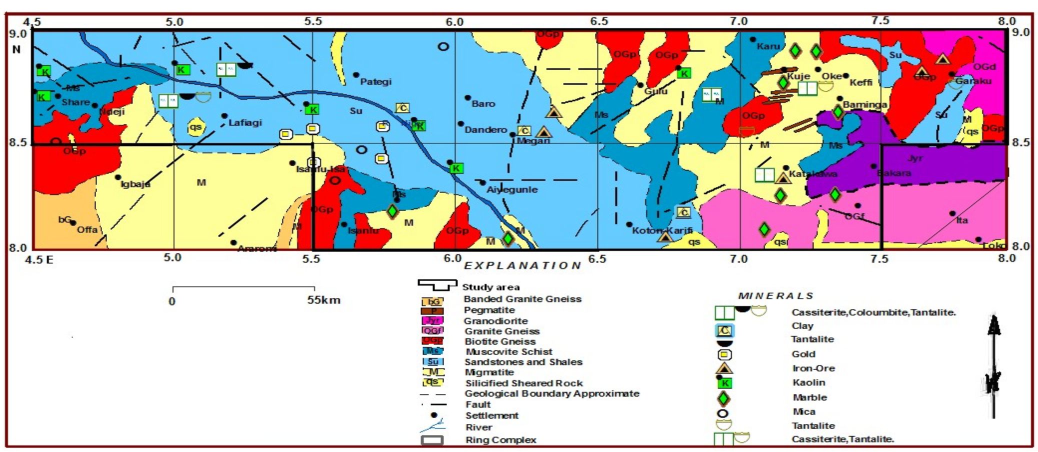

Fig. 2 Geological map of the study area (Adapted from the Geological map of Nigeria, 1996, Nigerian Geological Survey Agency)

MATERIALS AND METHODS

Materials

Data acquisition and analysis: The study area is made up of 11 aeromagnetic maps acquired from the Nigerian Geological Survey Agency. These are numbers: 202–208 and 225–228. The magnetic information consists of profiles or flight lines plotted on continuous strip chart. The aeromagnetic data was collected at a nominal flight altitude of 152.4 m along north–south flight lines spaced approximately 2 km apart. The airborne survey data were published in the form of ½ degrees by ½ degrees contour maps of total magnetic intensity on a scale of 1:100,000. The magnetic data was obtained from the digitization of total magnetic intensity contour maps at an interval of 0.0271 units (≈ 3 km) yielding 2,937 data points for the 11 sheets. The 3 km grid interval imposed a Nyquist frequency of 0.167 km^{-1}.

Methods

Regional-residual separation: The study area does not have complex geology and it has spatial extent, thus, it seemed plausible to assume that the regional field is a first-order polynomial surface. The regional magnetic field data was separated from the residual magnetic field data using the Robust Polynomial Fitting method. Residual magnetic field data was obtained as the deviations of the fitted plane surface from the total magnetic intensity.

Fractal–depth technique: The Spector and Grant (1970) method relates average depth to source to rate of decay of the magnetic power spectra. This method, which assumes a uniform distribution of parameters for an ensemble of magnetized blocks, leads to a depth dependent exponential rate of decay. Fedi *et al.* (1997) showed that also inherent in the model is a power law rate of decay that is independent of depth. Thus, for most cases, except for extreme depths and some block sizes, the observed power spectrum should be corrected for a power decay rate of $\beta \sim 3$. β is the decaying exponent. This power law decay rate is similar to the scaling behaviour supposed as a fractal character, of observed residual magnetic fields (Lawal *et al*., 2007).

Fractal geophysics supposes that many geophysical data sets have power law spectra. These include surface gravity and magnetics. Similarly, fractal geology; supposes that many geological phenomena are scale invariant, examples include frequency size distribution of rock fragments, faults, earthquakes, volcanic eruptions, mineral deposits and oil fields. Fractal distributions are used as a means of quantifying self-similar dispersions. A fractal distribution requires that the number of objects larger than a specified size has a power law dependence on the size (Turcotte, 1992).

The essential feature of a fractal is the existence of a similar structure at all length of scales. This is because the spatial variation of most geophysical parameters such as density and susceptibility often look similar at a wide range of scale; they can therefore be described using fractals (Bansal and Dimri, 2005, Sunmonu and Dimri, 2001, Lawal *et al*., 2007, Dimri, 1998, Gragnon *et al*., 2003, Todoeshcuck *et al*., 1992).

Maus and Dimri (1995) used the fractal method and modeled the sources of the potential field by a random function with scaling properties, defined on a half space with its top at a specified depth beneath the observation plane. This model has been shown by Maus and Dimri (1996) not to produce reliable depth results when applied to real data. Maus and Dimri (1996) observed that the theoretical power spectrum for a basin with source free sediments falls off rapidly at high frequency whereas the power spectra of real data tend to have flat tails.

According to Pilkington and Todoeshcuck (1998), the process of downward continuation corrects for the difference between the power spectra observed at the survey height and that at the ground. When magnetic data are continued downwards, the depth at which the power spectrum flattens out, termed the white depth can be taken as estimate of the depth to the magnetic source distribution (Hahn *et al*., 1976). This is equivalent to the depth evaluation procedure for an ensemble of magnetic sources introduced by Spector and Grant (1970). If survey height h = 0, the power spectrum becomes constant, under the assumption of uncorrelated magnetization values, and have a magnetization power spectra that is flat or white.

Thus, if a non–magnetic sedimentary stratum overlies a more magnetic crystalline basement, the depth to basement can be calculated from aeromagnetic data by using this method. The results obtained by Hahn *et al*. (1976) indicated that the spectrum becomes flat only when some sort of correlation in magnetization was assumed. The source scaling exponent γ reflects the degree of correlation in magnetization in a fractal model (Maus and Dimri, 1994, Pilkington and Todoeshcuck, 1990, 1998).

when
$\gamma = 0$
We have white noise, where values of magnetization are uncorrelated.

when
$\gamma > 0$
The values are anti-correlated in that successive values are likely to have opposite signs.

when
$\gamma < 0$

The values are correlated to a degree that increases with decreasing γ.
Pilkington *et al.* (1994) have shown that a correlated fractal model ($\gamma < 0$), of the crustal magnetization distribution is preferred over the standard assumption of independent, spectrally white magnetization distribution ($\gamma = 0$).

This study utilizes a fractal depth method which enables the prediction of the value of the scaling exponents at the source level without previous knowledge of the source depth. The method is applied to the 22 fractal subsections covering the study area, shown in Table 1. The residual magnetic field data for each subsection was continued downwards nine levels from 0.5 km down to 4.5 km at 0.5 km interval. At each of these levels the magnetic field scaling exponent β is determined by plotting log power against log frequency (Pilkington and Todoeshcuck, 1998, Gagnon *et al*., 2003).

The scaling exponent of the source is obtained by using the method of (Maus and Dimri, 1994 and Lawal *et al.*, 2007):

$\gamma = \beta + 1$ 1
where

β = scaling exponent of the field
γ = scaling exponent of the source
Applying a linear equation format and incorporating the depth of downward continuation, this gives
$\gamma = qd + r$ 2
where
d = depth of downward continuation
r and q are constants
In addition, Maus *et al.* (1997) assumed magnetic anomalies to be measured on a horizontal plane at an elevation z_t above magnetic sources. Magnetic sources are assumed to reside within a horizontal slab of

Table 1: 22 fractal subsections covering the study area

Subsection	Sheet name	Sheet number	Longitude (Decimal degrees)	Latitude (Decimal degrees)
1	Share	202	4.50 – 4.75	8.50 – 9.00
2	Share	202	4.75 – 5.00	8.50 – 9.00
3	Lafiagi	203	5.00 – 5.25	8.50 – 9.00
4	Lafiagi	203	5.25 – 5.50	8.50 – 9.00
5	Pategi	204	5.50 – 5.75	8.50 – 9.00
6	Pategi	204	5.75 – 6.00	8.50 – 9.00
7	Baro	205	6.00 – 6.25	8.50 – 9.00
8	Baro	205	6.25 – 6.50	8.50 – 9.00
9	Gulu	206	6.50 – 6.75	8.50 – 9.00
10	Gulu	206	6.75 –7.00	8.50 – 9.00
11	Kuje	207	7.00 – 7.25	8.50 – 9.00
12	Kuje	207	7.25 – 7.50	8.50 – 9.00
13	Keffi	208	7.50 – 7.75	8.50 – 9.00
14	Keffi	208	7.75 – 8.00	8.50 – 9.00
15	Isanlu	225	5.50 – 5.75	8.00 – 8.50
16	Isanlu	225	5.75 – 6.00	8.00 – 8.50
17	Aiyegunle	226	6.00 – 6.25	8.00 – 8.50
18	Aiyegunle	226	6.25 – 6.50	8.00 – 8.50
19	Koton karfi	227	6.50 – 6.75	8.00 – 8.50
20	Koton karfi	227	6.75 –7.00	8.00 – 8.50
21	Katakwa	228	7.00 – 7.25	8.00 – 8.50
22	Katakwa	228	7.25 – 7.50	8.00 – 8.50

thickness Δz, with magnetization oriented parallel or antiparallel to the geomagnetic field. Magnetization is thus assumed to be a random function of position (x, y, z), with a power spectrum proportional to the norm of the wave number raised to power $-\beta$ (fractal parameter or field scaling exponent).Hence, Bouligand *et al.* (2009) and Maus *et al.* (1997) suggested that magnetization has a fractal distribution defined by three independent parameters: the depths to the top and bottom of magnetic sources and a fractal parameter β related to the geology.

The fractal parameter β, which is the slope of the power spectrum in a log–log scale, is related to the geology and thus might vary geographically depending on rock types or geologic structures. With these assumptions, the magnetic sources can be fully described by three unknowns: the depth to the top of magnetic sources z_t, the thickness of magnetic sources Δz, and the fractal parameter β (Bouligand *et al.,* 2009). Assuming a constant value of $\beta = 4$ (Maus *et al.*, 1997); the depth to the bottom of magnetic sources z_b is deduced from the depth to the top (z_t) and the thickness (Δz) (Bouligand *et al.,* 2009).

$$z_b = z_t + \Delta z \qquad 3$$

Two dimensional modeling of the residual magnetic field anomalies:
Figure 3 shows six profiles AA^1, BB^1, WW^1, KK^1, DD^1 and PP^1 drawn across residual magnetic field anomalies; superimposed on the geology map. The susceptibility values used for modeling the residual magnetic anomalies are: sedimentary rock section (0.0 gaussian units) and basement rock section (0.0013–0.005 gaussian units). Remanence adopted is about 33,000 nano tesla, Inclination = –7.0 ^{0} and Declination = – 4.0 ^{0}, adapted from Udensi and Osazuwa (2002). The depth–to–top of magnetic sources results obtained from the fractal depth technique was used as constraint for modeling the residual magnetic field anomalies.

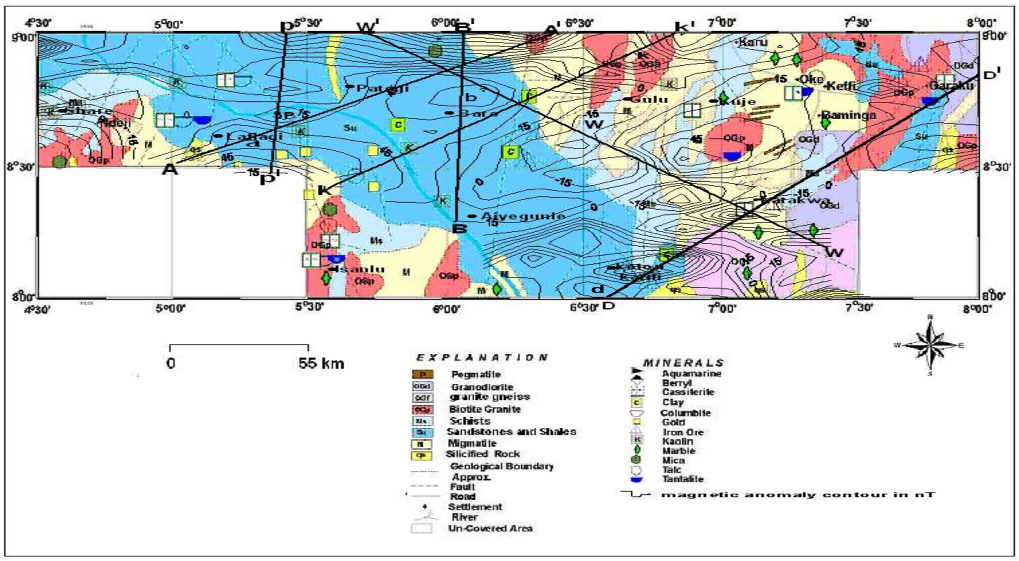

Fig. 3: Map of profiles for modeling. Contour interval = 15 nano tesla (nT)

RESULTS
The total magnetic intensity (TMI) map of the study area is shown in Figure 4. The general trending fabric of the magnetic anomalies is the northeast–southwest direction. Additionally, Figure 5 shows the TMI highs (H) and lows (L). The magnetic highs are dominant in the eastern, north–eastern, south–eastern, south–central, northern, western and west–central parts of the map. While magnetic lows are predominant in the northern, central and southern sections of the survey area.

Sedimentary rocks are mostly characterized by low susceptibility values. However, Figure 6 shows the area covered by sedimentary rocks; that is the southern Bida basin section; to be characterized by low, medium and high TMI anomalies, with high TMI observed mainly at its central part, trending in a northeast–southwest direction. The high TMI values may result from iron stones within the sedimentary pile, buried magnetic materials such as buried steel casings or from basement rock uplift beneath the sedimentary rocks caused by highly magnetic basic igneous intrusions.

The regional magnetic field map (Figure 7) shows contour lines trending in a general northwest–southeast direction. The residual magnetic field map (Figure 8) shows a general trending fabric of northeast–southwest direction similar to those of the total magnetic intensity map (Figure 4). To obtain the values for γ, β and depth–to–top of magnetic sources z_t, a Fortran programme, Fractal; was applied to the downward continued data of the 22 subsections. Figure 9 is a sample plot which shows that the field scaling exponent varies linearly with depth of downward continuation.

The depth–to–top of magnetic sources z_t for all the subsections is shown in Table 2. The depth–to–top of magnetic sources ranges from 0.022 km to 3.88 km with an average value of 1.299 km. The highest fractal depth to source of 3.88 km is observed in subsection 4. While the lowest fractal depth to source of 0.022 km is observed in subsection 21. Figure 10 shows low depth–to–top of magnetic sources at Isanlu, Kuje, Gulu, Karu, and Katakwa (basement rock sections). While the higher values of z_t are observed at Aiyegunle, Lafiagi and Pategi (basin areas). The surface relief map, Figure 11 depicts a fold pattern indicating the topography of the basement rocks.

Depth-to-bottom of magnetic sources (Z_b): Table 3 shows the results obtained for Z_b (depth–to–bottom of magnetic sources) and Δz (thickness of magnetic anomaly within the crust). The values of Z_b ranges from 8.364 km to 15.094 km with an average value of about 11.837 km. Figure 12 shows coloured representation of depth–to–bottom of magnetic sources. It indicates high values of Z_b around Pategi and Aiyegunle, while low values of Z_b are observed around Garaku and Katakwa.

The source scaling exponent γ ranges from 1.541 to 3.809 with an average value of 2.806. Figure 13 shows high values of γ around Gulu, Karu and Koton Karifi which are predominantly basement rock sections. While low values of γ are observed around Lafiagi, Pategi and Aiyegunle which are basin dominated areas.

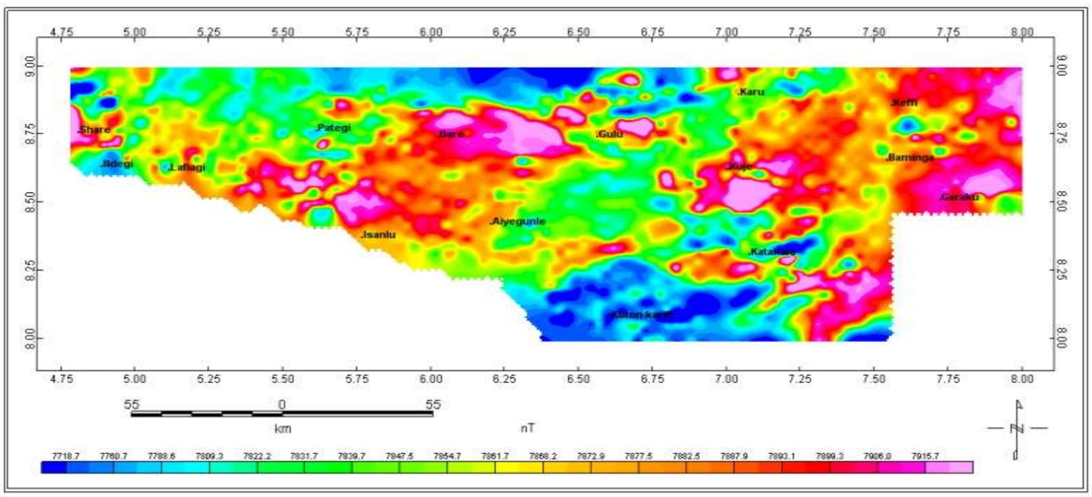

Fig. 4. Total magnetic intensity map of the study area

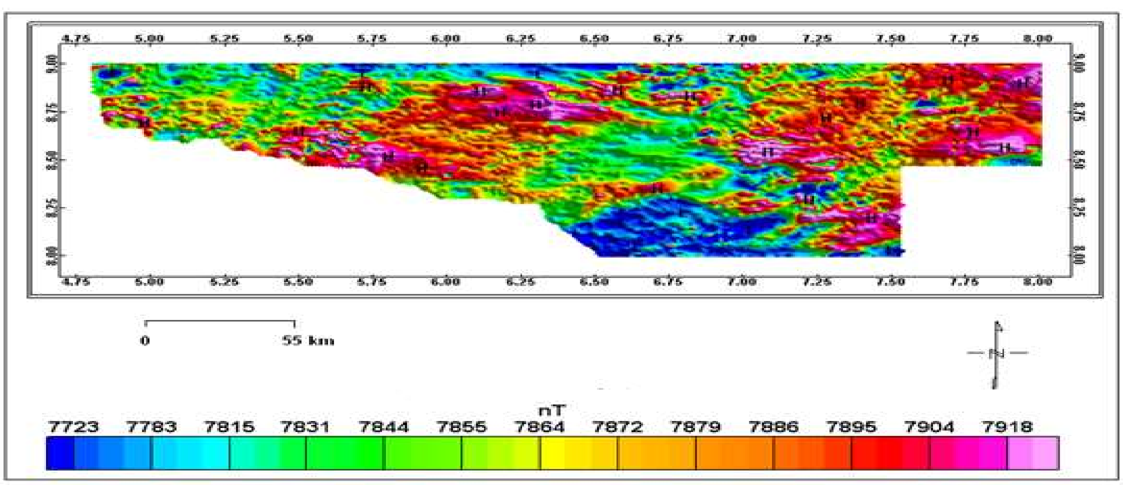

Fig. 5. Total magnetic intensity map of the study area showing areas of magnetic highs (H) and lows (L)

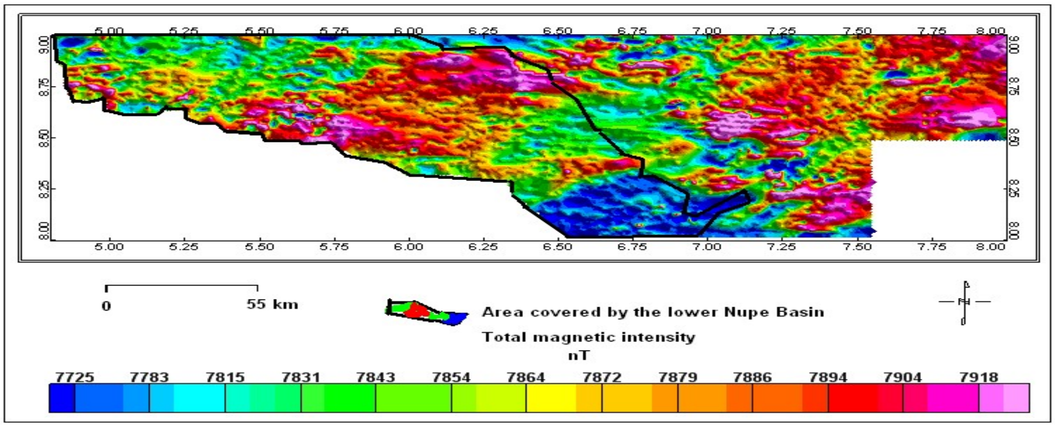

Fig. 6. Delineation of the area covered by the southern Bida basin using the total magnetic intensity map

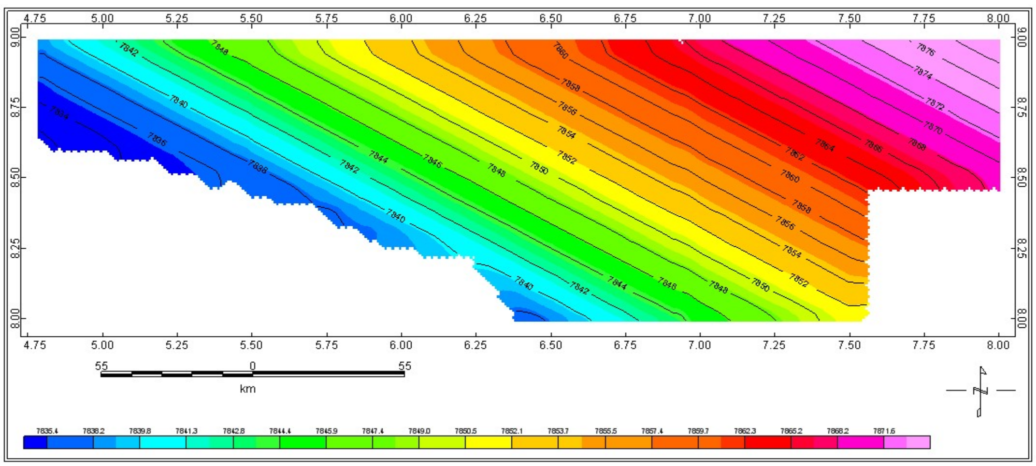

Fig. 7. Regional magnetic field map of the study area. Contour interval = 2 nT

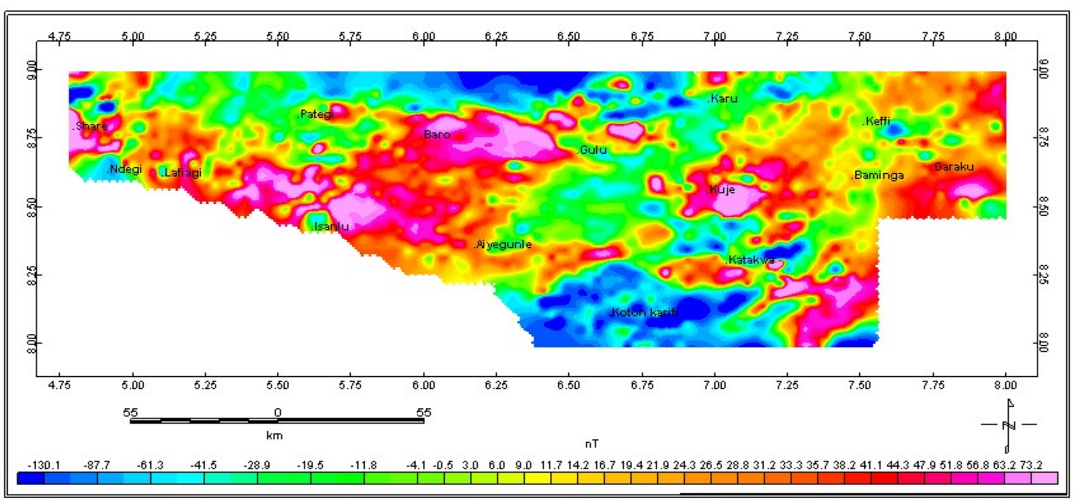

Fig. 8. Residual magnetic field map of the study area

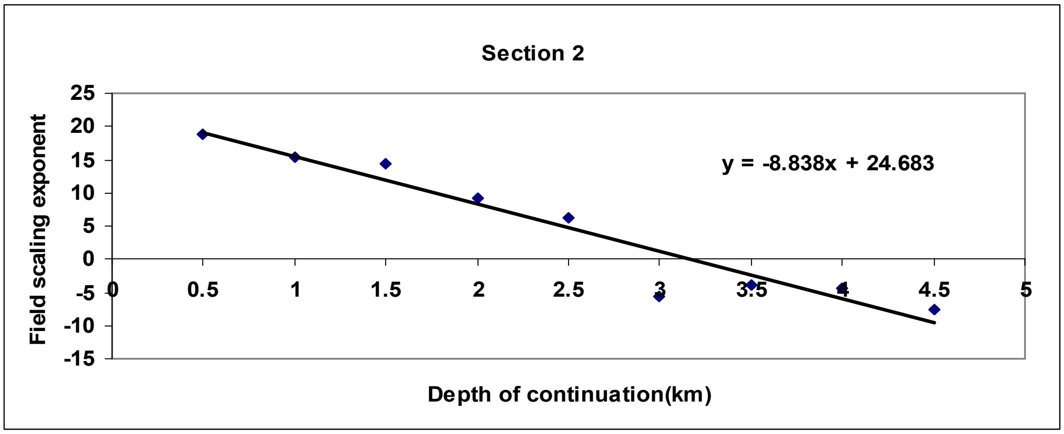

Fig. 9. Variation of β with depth of downward continuation (0.5 km – 4.5 km at 0.5 km interval)

Table 2: Depth–to–top of magnetic sources (z_t) and the source scaling exponent γ for the 22 fractal subsections

Subsection	Longitude (Decimal degrees)	Latitude (Decimal degrees)	Depth–to–top of magnetic source (km)	Source scaling exponent γ
1	4.625	8.75	No data	No data
2	4.905	8.75	2.510	3.500
3	5.125	8.75	3.400	1.541
4	5.375	8.75	3.880	2.226
5	5.625	8.75	2.642	2.440
6	5.875	8.75	1.620	2.610
7	6.125	8.75	1.020	2.930
8	6.375	8.75	0.568	1.907
9	6.625	8.75	0.085	3.632
10	6.875	8.75	0.038	3.809
11	7.125	8.75	0.044	3.579
12	7.375	8.75	0.076	3.765
13	7.625	8.75	0.114	3.588
14	7.875	8.75	0.065	3.744
15	5.625	8.25	0.625	2.641
16	5.875	8.25	1.244	1.686
17	6.125	8.25	3.715	2.087
18	6.375	8.25	3.468	3.320
19	6.625	8.25	1.820	3.017
20	6.875	8.25	0.225	2.200
21	7.125	8.25	0.022	2.462
22	7.375	8.25	0.092	2.237

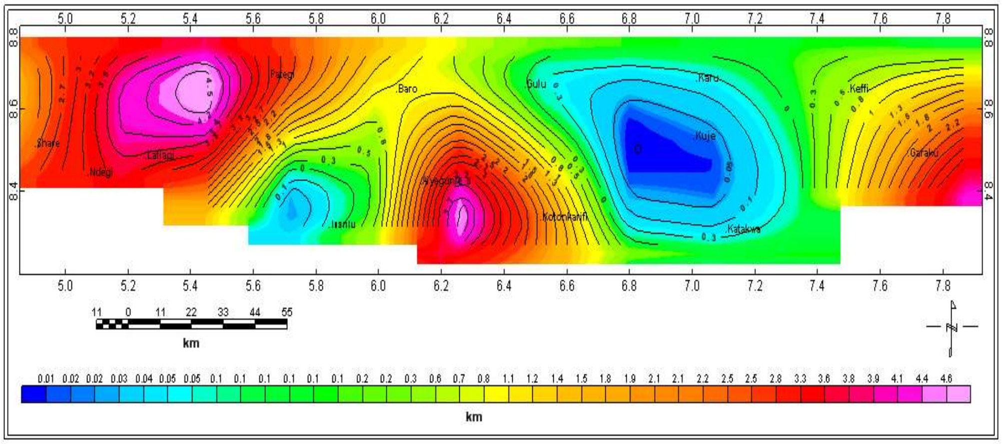

Fig. 10. Fractal depth-to-top of magnetic sources. Contour interval = 0.01 km

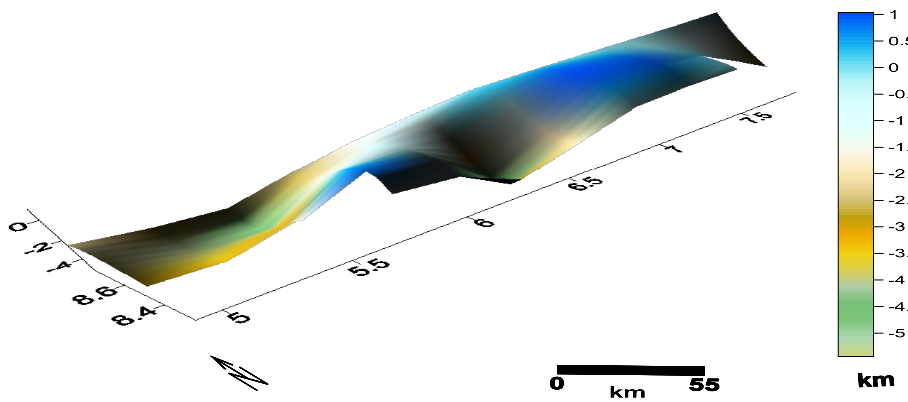

Fig. 11. Surface relief map of fractal depth-to-top of magnetic sources (z_t)

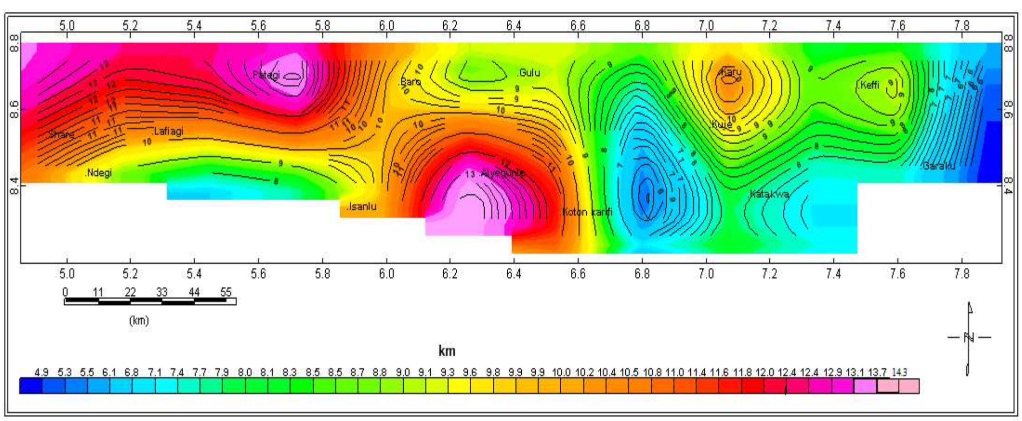

Fig. 12. Fractal depth–to–bottom of magnetic sources. Contour interval = 0.5 km

Table 3: Depth-to-bottom of magnetic source (Z_b) and thickness of anomaly in the crust (Δz)

Longitude (Decimal degrees)	Latitude (Decimal degrees)	Z_b (km)	Δz (km)
4.625	8.750	No data	No data
4.905	8.750	15.044	12.534
5.125	8.750	14.520	11.120
5.375	8.750	14.600	12.452
5.625	8.750	15.094	11.652
5.875	8.750	12.494	10.874
6.125	8.750	10.092	9.072
6.375	8.750	11.801	11.233
6.625	8.750	10.929	10.844
6.875	8.750	10.329	10.291
7.125	8.750	11.672	11.628
7.375	8.750	10.316	10.240
7.625	8.750	10.640	10.526
7.875	8.750	8.364	8.298
5.625	8.250	11.030	10.405
5.875	8.250	12.485	11.241
6.125	8.250	14.778	11.063
6.375	8.250	13.418	9.950
6.625	8.250	12.688	10.868
6.875	8.250	9.070	8.845
7.125	8.250	10.214	10.192
7.375	8.250	8.986	8.895

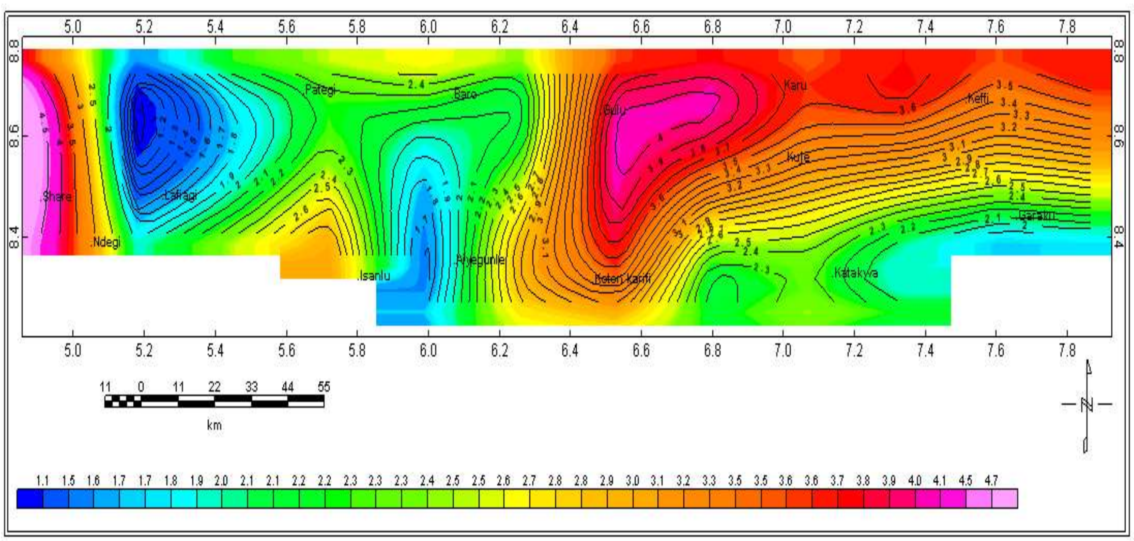

Fig. 13. Source scaling exponent. Contour interval = 0.1

Profile parameters and model results

(i) Profile AA[1]:

Profile AA[1] is a northeast–southwest line drawn across a northwest-southeast trending anomaly (a) located in the western part of the map around Lafiagi (Figure 3). The profile cuts across the width of the sedimentary section flanked by basement complex rocks on both sides. The profile length is about 80 km. Figure 14 shows sedimentary rock thicknesses ranging from 0.0 km to 0.94 km.

(ii) Profile BB[1]:

Profile BB[1] is a vertical line drawn across an east-west trending anomaly (b) situated in the northern section of the map around Baro (Figure 3). The part of the map covered by the profile is majorly made up of sedimentary rocks. The profile length is about 77 km. Figure 15 shows sedimentary rock thicknesses ranging from about 0.11 km to 3.98 km. The inferred intrusive rock is situated at a depth of 2.05 km.

(iii) Profile KK[1]:

Profile KK[1] is a northeast-southwest line drawn across a northwest-southeast trending anomaly (k) located in the northern part of the map (Figure 3). The profile cuts across the width of the sedimentary section flanked by basement complex rocks on both sides. The profile length is about 80 km. Figure 16 reveals sedimentary rock thicknesses ranging from 0.0 km to 0.52 km. The deduced intrusive rocks are situated at depths of 1.27 km, 1.13 km and 1.17 km respectively.

(iv) Profile PP[1]:

Profile PP[1] is a vertical line drawn across an east-west trending anomaly (p) located in the northwestern section of the map (Figure 3). The section of the map covered by the profile is mainly made up of sedimentary rocks. The profile length is about 60 km. Figure 17 indicates sedimentary rock thicknesses ranging from 0.09 km to 3.92 km.

(v) Profile WW[1]:

Profile WW[1] is a northwest-southeast line drawn across a northeast-southwest trending anomaly (W) located in the central part of the map (Figure 3). The section of the map covered by the profile is partly made up of basement complex rocks and partly sedimentary rocks. The profile length is about 130 km. Figure 18 shows sedimentary rock thicknesses ranging from 0.0 km to 2.07 km. The deduced intrusive rock is situated at a depth of 3.78 km.

(vi) Profile DD[1]:

Profile DD[1] is a northeast-southwest line drawn across a northwest-southeast trending closure (d) located in the southern part of the map (Figure 3). The section of the map covered by the profile is partly made up of basement complex rocks and partly sedimentary rocks. The profile length is about 120 km. Figure 19 reveals sedimentary rock thicknesses ranging from 0.0 km to 1.44 km. The inferred intrusive rock is situated at a depth of 1.02 km.

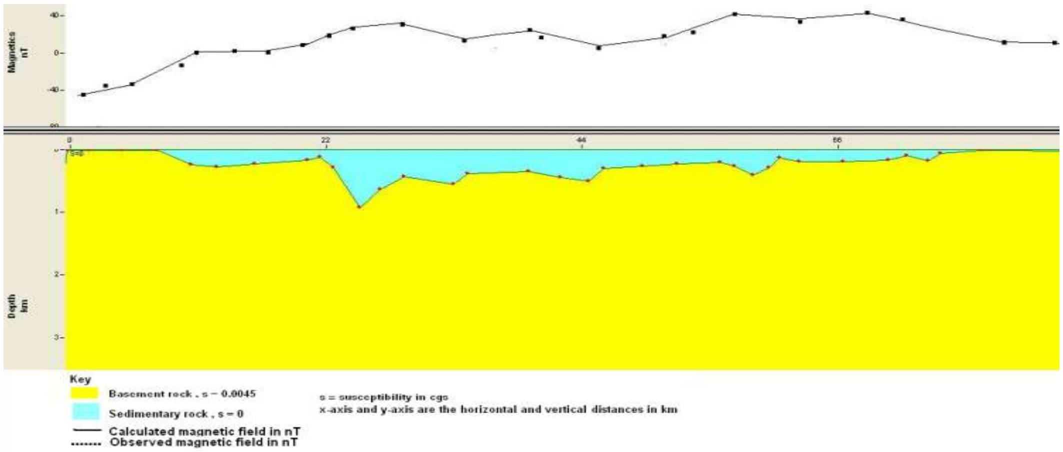

Fig. 14 Profile AA[1] model

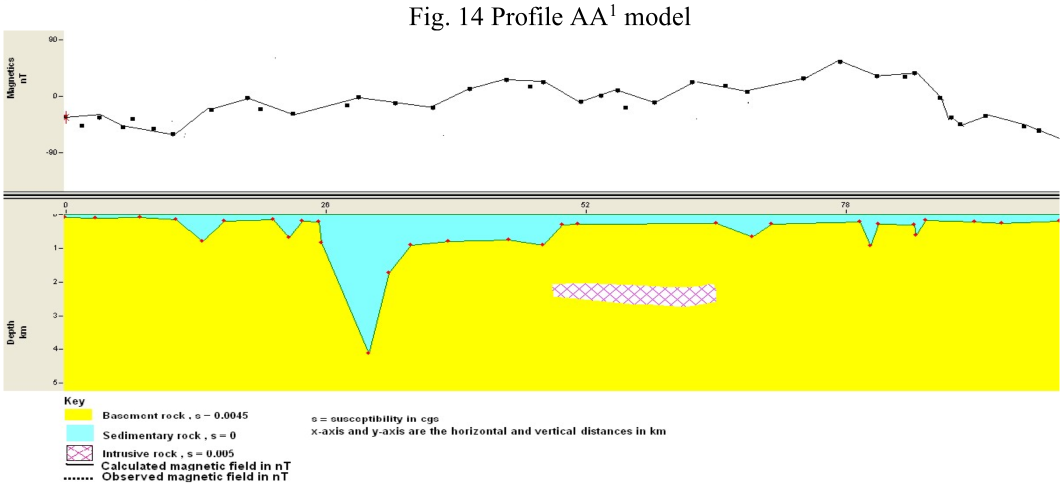

Fig. 15 Profile BB[1] model

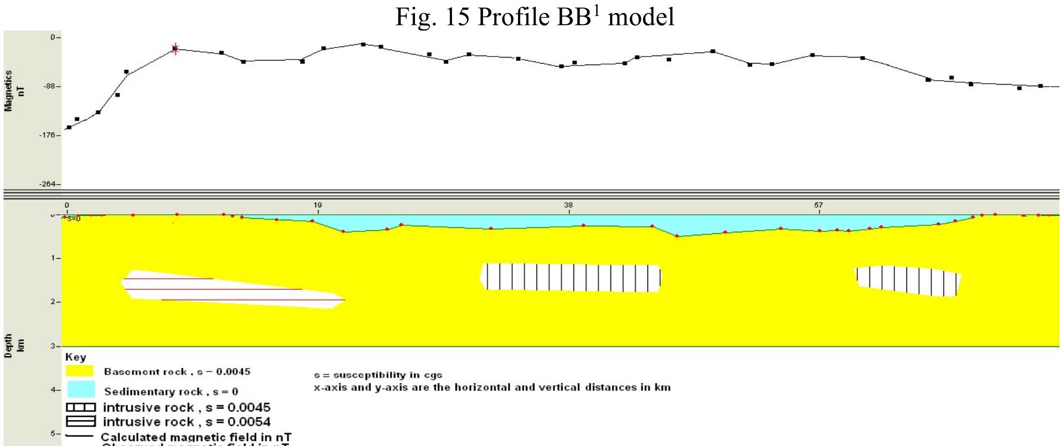

Fig. 16 Profile KK[1] model

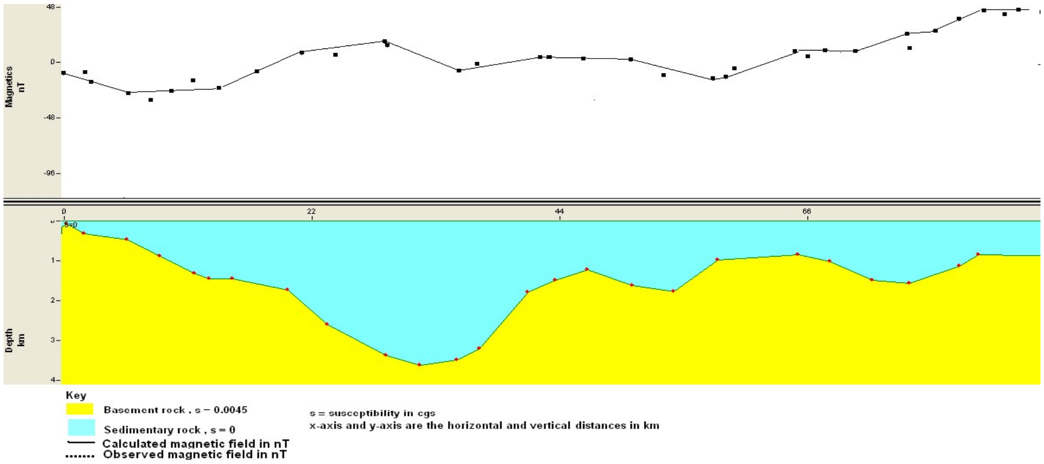

Fig. 17 Profile PP[1] model

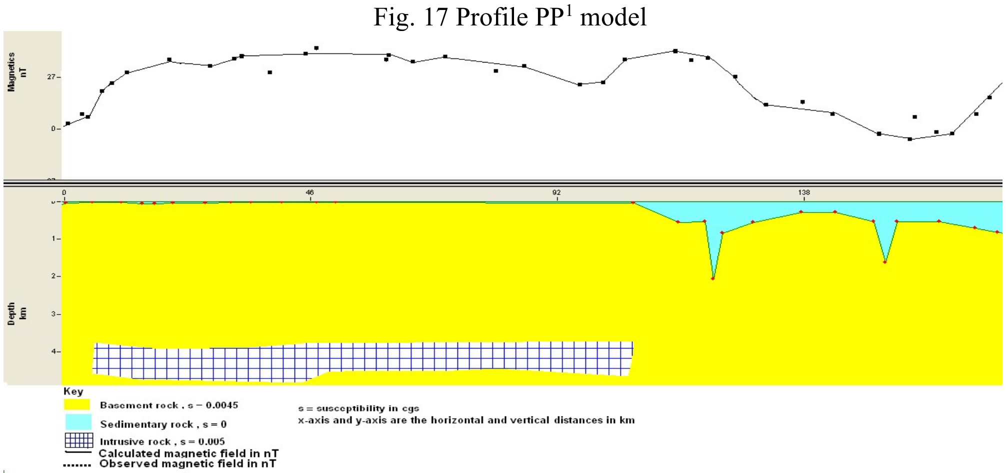

Fig. 18 Profile WW[1] model

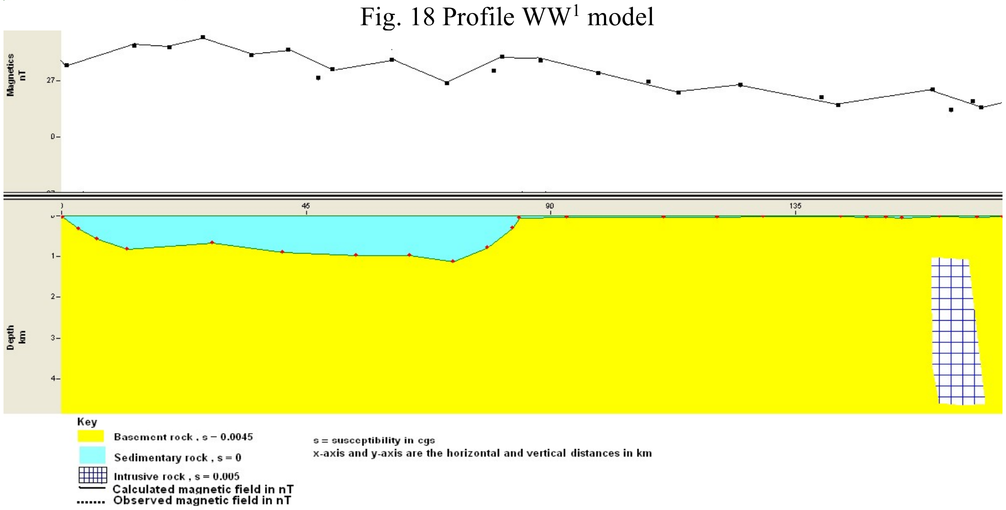

Fig. 19 Profile DD[1] model

DISCUSSION

High Fractal depth z_t are prominent around Share, Lafiagi, Aiyegunle, Pategi and Ndegi, Figure 20 (a and b). These areas are predominantly made up of sedimentary rocks. The highest z_t of 3.88 km was obtained from subsection 4 around Lafiagi. Since sedimentary rocks exhibit very low susceptibility values, magnetic sources within the research area; thus originate mainly from the basement rocks underlying the sediments.

Low z_t are observed around Gulu, Kuje, Karu, Garaku, Keffi, Katakwa and Isanlu. These areas are predominantly made up of basement rocks. These rocks comprise of units including biotite granites which are not deeply placed, thus accounting for the low z_t values. Thus, z_t depicts the basement rock topography.

High source scaling exponent γ are observed around Gulu, Karu and Keffi, Figure 20 (a and c). These areas are dominated by basement rocks. While, low γ are observed around Aiyegunle and Lafiagi areas; mainly made up of sedimentary rocks. Thus, it is suggested that source scaling exponent distinguishes the basin from basement rock sections.

The sedimentary rock thickness obtained from the six models ranges from a minimum of 0.0 km to a maximum of about 3.98 km. The modeling results showed that the study area has intrusive rocks at various depths not less than 1.02 km. The inferred spread of sedimentary thicknesses in the study area is shown in Figure 21. The diagram highlights the thickest portion of the study area around Aiyegunle in the south central part of the survey area, with a thickness of 3.98 km.

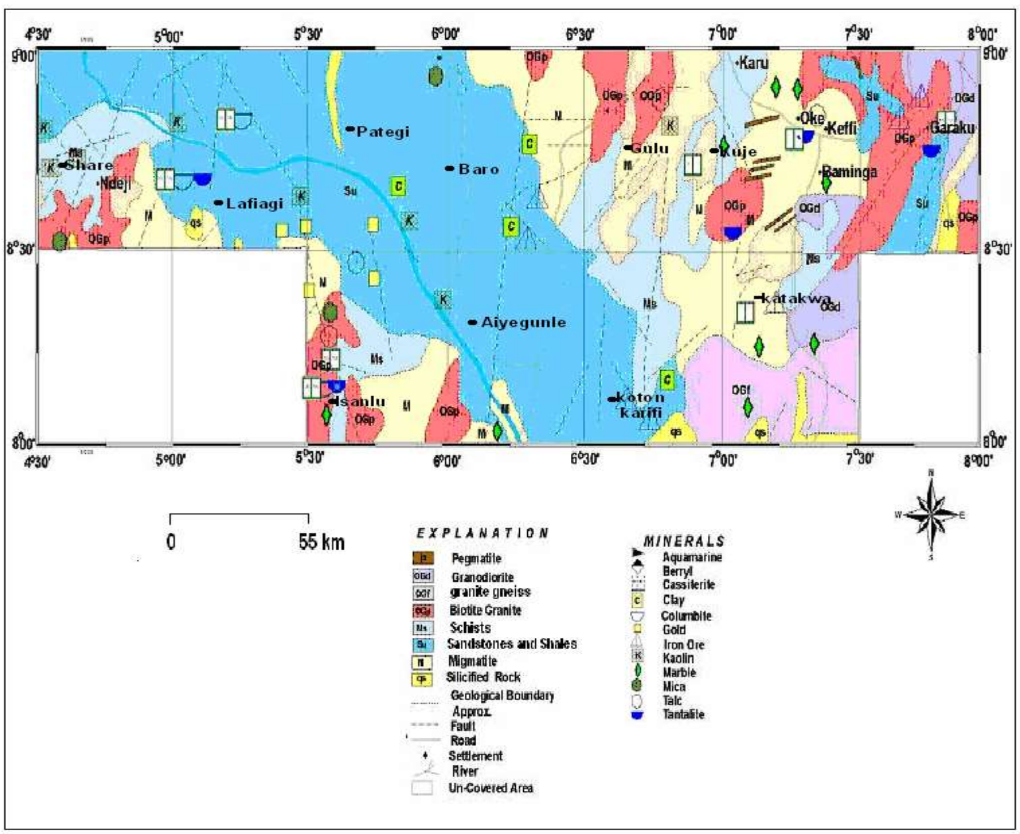

(a) Geological map of the study area

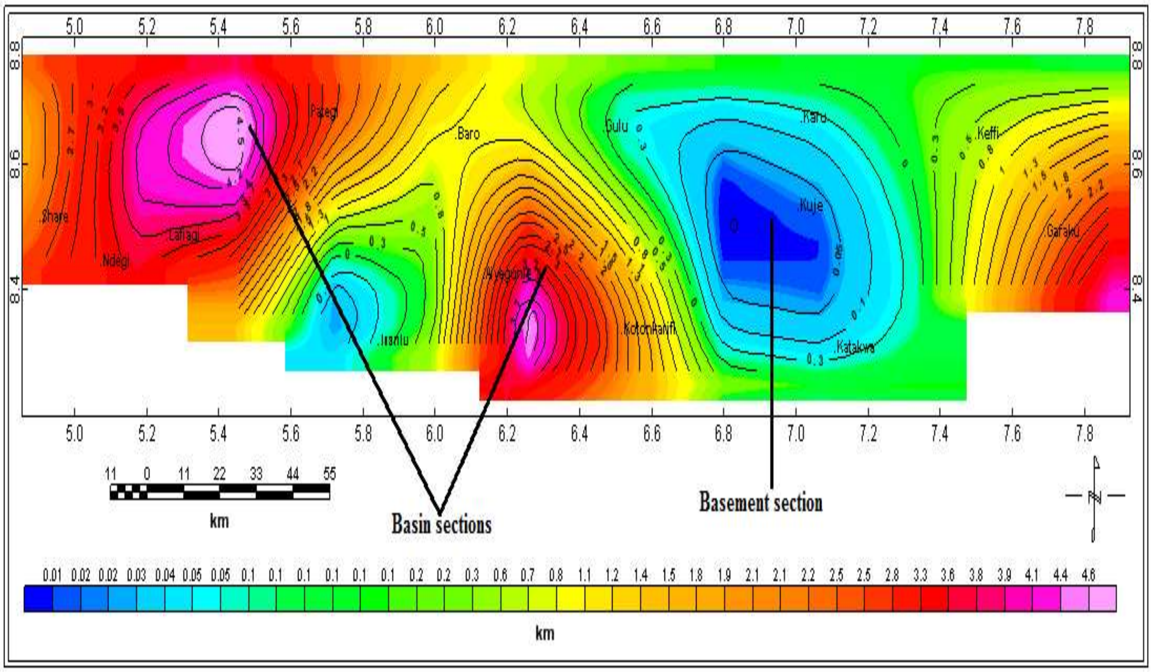

(b) Fractal depth to top of magnetic sources map

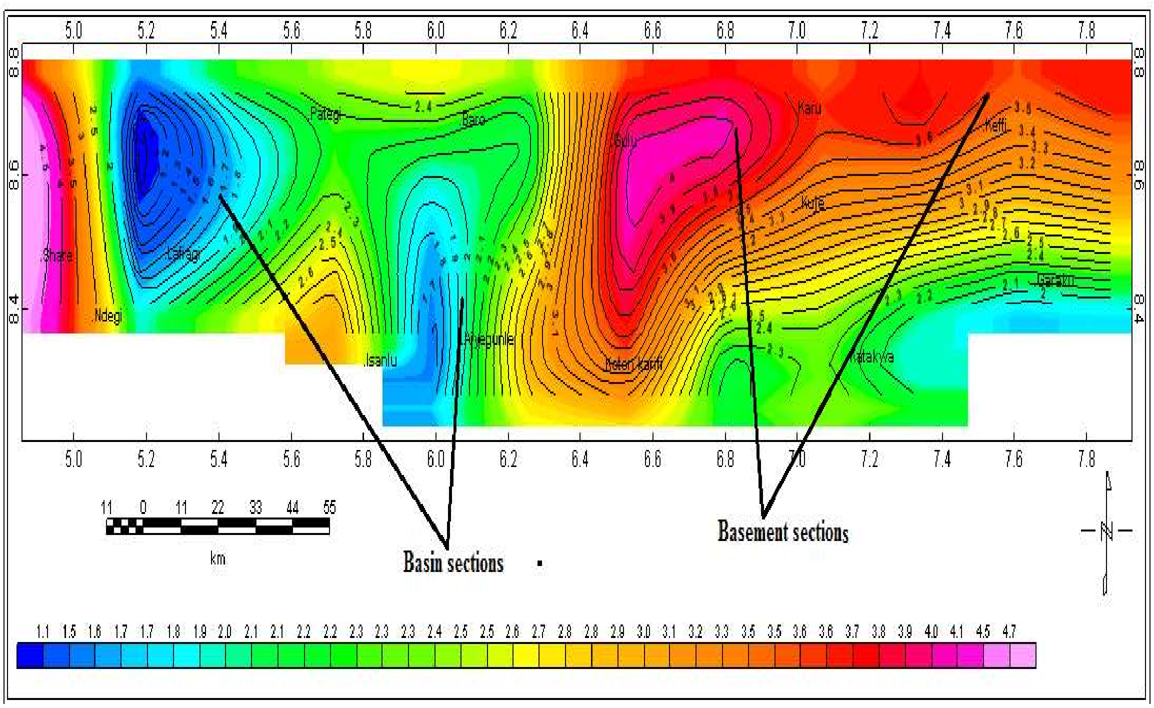

(c) Source scaling exponent

Fig. 20: Geology of the study area, depth-to-top of magnetic sources and source scaling exponent

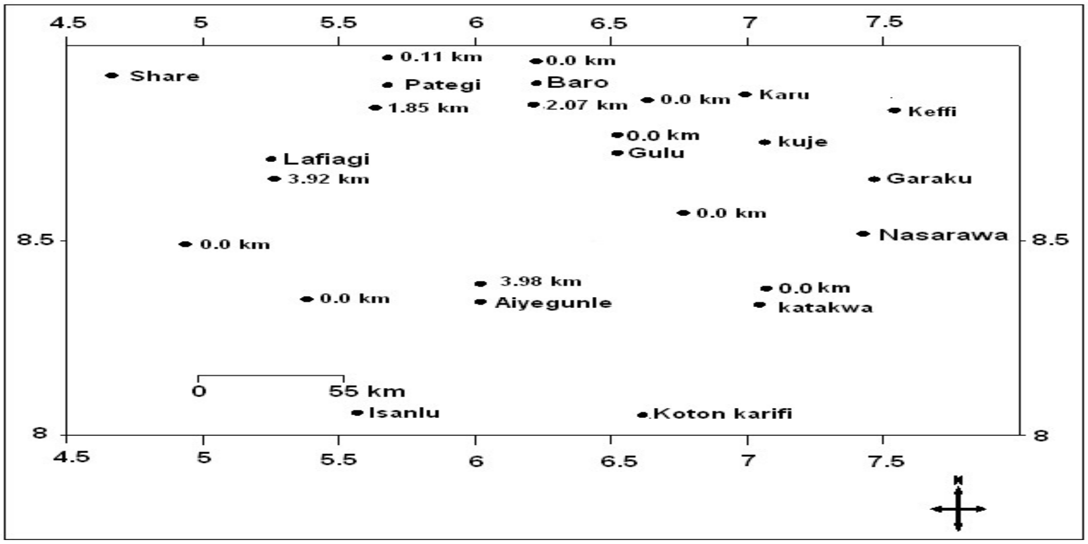

Fig. 21 Sedimentary thicknesses inferred from modeling of residual magnetic field anomalies, depicting the basement topography of the survey area.

CONCLUSION

Magnetic high contour closures are prominent around Garaku, Katakwa and Koton Karifi areas where there are occurrences of iron ore. Magnetic high anomalies are also noticeable around Ndegi, Gulu, Garaku and Keffi sections where there are occurrences of biotite granite rocks. Furthermore, the study showed that several basic igneous intrusions characterize the research area at depths not less than 1.02 km. The deepest placed intrusion was inferred to be at a depth of 3.78 km. Basement rock uplift deduced at the central portion of the Bida basin section may be due to basic igneous intrusions.

The field scaling exponent varies linearly with depth of downward continuation, and the source scaling exponent delineates the basement and basin sections. Basement rock topography deduced from the fractal depth method depicts a fold pattern having the highest sedimentary thickness of 3.88 km around Lafiagi, which is in agreement with the 3.92 km obtained from modeling profile PP^1. However, the thickest point was observed around Aiyegunle (south central section of the survey area) with a value of 3.98 km. Thus, hydrocarbon accumulation may be enhanced by the high thickness of sediments at both Lafiagi and Aiyegunle areas.

ACKNOWLEDGEMENTS

The authors are grateful to the staff of Physics Department, Federal University of Technology, Minna and the staff of the Nigerian Geological Survey Agency, Abuja, Nigeria for their invaluable assistance in various capacities.

REFERENCES

Akande, S. O., Ojo, O. J., Erdtmann, B. D. & Hetenyi, M. (2005).Paleoenvironments, organic petrology and rock–eval studies on source rock facies of the Lower Maastrichtian Patti Formation, southern Bida Basin, Nigeria. *Journal of African Earth Sciences,* 41,394–406.

Bansal, A. R. & Dimri, V. P. (2005). Depth determination from a non–stationary magnetic profile for scaling geology. *Geophysical Prospecting,* 53,399–410.

Braide, S. P. (1990). Sedimentation and tectonics in the southern Bida Basin, Nigeria. Depositional response to varying tectonic context. *American Association of Petroleum Geologists (AAPG) Bulletin,* 74, 1–20.

Bouligand, C., Jonathan, M., Glen, G. & Blakely, R. J. (2009). Mapping Curie temperature depth in the western United States with a fractal model for crustal magnetization. *Journal of Geophysical Research,* 114, 1–25.

Dimri, V. P. (1998). Fractal detectability limits of geophysical surveys. *Geophysics,* 2, *1943–1946.*

Fedi, M., Quarta, T. & Santis, A. D. (1997). Inherent power law behaviour spectra from a Spector and Grant ensemble. *Geophysics,* pp. 1143–1150.

Gragnon, J. S., Lovejoy, S. & Schertzer, D. (2003). Multifractal surfaces and terrestrial topography. *Europhysics Letters,* 62, 801–807.

Hahn, A., Kind, E. G. & Mishra, D. C. (1976). Depth estimation of magnetic sources by means of Fourier amplitude spectra. *Geophysics,* 24,287–308.

Lawal, K. M., Umego, M. N. & Ojo, S.B. (2007). Depth to basement mapping using Fractal technique: application to the Chad Basin, northeastern Nigeria. *Nigerian Journal of Physics,* pp.75–88.

Maus, S. & Dimri, V. P. (1994). Scaling exponents of potential fields due to scaling Sources. *Geophysics Research Letters,* 21, 89–894.

Maus, S. & Dimri, V. P. (1995). Potential field power spectrum inversion for scaling Geology. *Journal of Geophysics Research,* 100, 12605–12616.

Maus, S. & Dimri, V. P. (1996). Depth estimation from the scaling power of potential fields. *Geophysical Journal International,* 124, 113–120.

Maus, S., Gordon, D. & Fairhead, D. (1997). Curie temperature depth estimation using a self-similar magnetization model. *Geophysical Journal International,* 129, 163– 168.

Obaje, N. G. (2009). *Geology and mineral resources of Nigeria*. Berlin: Springer Publishers, pp. 1–203.

Pilkington, M., Gregotski, M. E. & Todoeshcuck, J. P. (1994). Using fractal crustal magnetization models in magnetic interpretation. *Geophysical prospecting* 42, 677–692.

Pilkington, M. & Todoeshcuck, J. P. (1990). Stochastic inversion for scaling geology. *Geophysical Journal International,* 102,205–217.

Pilkington, M. & Todoeshcuck, J. P. (1998). Use of fractals in potential field interpretation. *Canadian Geophysical Society,* pp. 1–2.

Shekwolo, P. D. (1992). Regional hydrogeology of Bida Basin, Ph.D. Thesis, Ahmadu Bello University, Zaria, Nigeria.

Smith, R. S., Thurston, J. B., Dai, T. and MacLeod, I. N. (1998). iSPI–the improved source parameter imaging method: Geophys. Prosp. 46: 141–151.

Spector, A. & Grant, F. S. (1970). Statistical models for interpreting aeromagnetic data. *Geophysics,* 35, 293–302.

Sunmonu, L. A. & Dimri, V. P. (2001). Multifractal analysis and seismicity of the Himalayan Region–a case study. *Nigerian Journal of Physics,* 13, 106–111.

Thurston, J. B. and Smith, R. S. (1997). Automatic conversion of magnetic data to depth, dip, and susceptibility contrast using the SPI method: Geophysics, 62: 807–813.

Thurston, J. B., Smith, R. S. and Gillon, J. (2002). A multimodel method for depth estimation from magnetic data, Geophysics, 67:555–561.

Todoeshcuck, J. P., Pilkington, M. & Gregotski, M. E. (1992). If geology is fractal, what do we do? *The Leading Edge,* pp. 29–35.

Turcotte, D. L. (1992). *Fractals and chaos in geology and geophysics*. New York: Cambridge University Press.

Udensi, E. E. & Osazuwa, I. B. (2002). Two and half dimensional modeling of the major structures underlying the Nupe Basin, Nigeria using aeromagnetic data. *Nigerian Journal of Physics.* 14, 56–61.